PCCP

Accepted Manuscript

ROYAL SOCIETY OF CHEMISTRY

www.rsc.org/pccp

Physical Chemistry Chemical Physics RSC Publishing

ARTICLE

Solvatochromic, Spectral, and Geometrical Properties of Nifenazone: A DFT/TD-DFT and Experimental Study

Abdulilah Dawoud Bani-Yaseen,[a,*] Mona Al-Balawi[b]

Page | 1Cite this: DOI: 10.1039/x0xx00000x

Received 00th January 2012,
Accepted 00th January 2012

DOI: 10.1039/x0xx00000x

www.rsc.org/

Solvatochromic, spectral, and geometrical properties of nifenazone (NIF), a pyrazole-nicotinamide drug, were experimentally and computationally investigated in several neat solvents and in hydro-organic binary systems such as water-acetonitrile and water-dioxane systems. The bathochromic spectral shift observed in NIF absorption spectra when reducing the polarity of the solvent was correlated with the orientation polarizability (Δf). Unlike aprotic solvents, a satisfactory correlation between λ_{max} and Δf was determined (linear correlation of regression coefficient, R, equal to 0.93) for polar protic solvents. In addition, the medium-dependent spectral properties were correlated with the Kamlet-Taft solvatochromic parameters (α, β, and π*) by applying a multiple linear regression analysis (MLRA). The results obtained from this analysis were then employed to establish MLRA relationships for NIF in order to estimate the spectral shift in different solvents, which in turn exhibited excellent correlation (R > 0.99) with the experimental values of ν_{max}. Density functional theory (DFT) and time-dependent DFT calculations theory coupled with the integral equation formalism-polarizable continuum model (IEF-PCM) were performed to investigate the solvent-dependent spectral and geometrical properties of NIF. Calculations showed good and poor agreements with the experimental results using the CAM-B3LYP and B3LYP functionals, respectively. Experimental and theoretical results confirmed that the chemical properties of NIF are strongly dependent on the polarity of the chosen medium and its hydrogen bonding capability. This in turn supports the hypothesis of the delocalization of the electron density within the pyrazole ring of NIF.

Keywords: Time-dependent density functional theory, integral equation formalism-polarizable continuum model, electronic absorption spectra, solvatochromism, hydro-organic binary system, multiple linear regression analysis, nifenazone

Introduction

Medium-dependent physical properties of drugs are increasingly regarded as a relevant aspect in the pharmaceutical research and industry. A large range of compounds, including drugs commonly used in everyday life, are medium-dependent, i.e., their activity may vary with the composition of the medium [1]. The physical properties of potential drugs, for example, may strongly depend on ultraviolet/visible radiations, the effect on biological systems being particularly interesting because of their potential uses in fields such as photosensitization [2]. In particular, photosensitization reactions involve various compounds, that have been the main topic of investigation in numerous studies aimed at improving the efficiency of photosensitizers [2-4] We would like to remark that the combination of hydrophobic and hydrophilic substituents in the structure of photosensitizers results in an intramolecular polarity axis that can increase the sensitivity of the properties of the medium [4]. In order to understand and predict the chemical behaviour of photosensitizers, a variety of photo-physicochemical studies needs to be carried out, including the investigation of the influence of the medium on the chemical properties of the photosensitizers, such as pH, ionic strength, and chemical composition of the medium [7].

Solvent-solute interactions include a diverse range of intermolecular forces that can modify the physicochemical behaviour of the solute. In this regard, solvatochromism is a technique that provides relevant details about the behaviour of drugs in environments of different polarities, and in particular, about solute–solvent interactions [8-14]. This point is crucial for the research and development of novel effective drugs, which is, of course, one of the main aims of the pharmaceutical industry. In addition, understanding the influence of medium properties can provide a powerful tool to control the severity of drug toxicity and the drug efficiency in biological systems.

Among the pharmaceuticals that exhibit strong medium dependent-properties, those containing an amide functional group, such as Nifenazone (NIF or N-(1,5-dimethyl-3-oxo-2-phenyl-2,3-dihydro-1H-pyrazol-4-yl) nicotinamide), that represents a very attractive class of compounds due to the combination of phenazone and nicotinamide properties [15-17]. Chemical structure of NIF is shown in scheme 1.

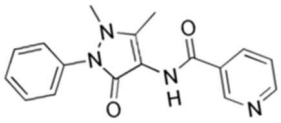

Scheme 1. Chemical Structure of Nifenazone

In this work, a mixed theoretical and experimental approach was employed in order to explore the influence of the medium on the solvatochromic, spectral, and geometrical properties of the pyrazole-nicotinamide drug NIF. In particular, the UV-Vis absorption spectra of NIF in neat and binary hydro-organic solvents of different polarity and hydrogen bonding capability were collected; density functional theory (DFT) and time-dependent DFT (TD-DFT) calculations at the B3LYP/6-31G+(d) level of theory coupled with integral equation formalism polarizable continuum model (IEF-PCM) were carried out. All experimental and computational results were interpreted and discussed in terms of the medium-dependent structural properties of NIF.

Experimental

Materials. NIF was purchased from Sigma-Aldrich and used as received. All solvents (methanol, ethanol, propanol, isopropanol, acetonitrile, ethylacetate, n-hexane, chloroform, 1,4-dioxane, dimethylformamide (DMF), and dimethylsulfoxide (DMSO)) were of spectrophotometeric grade and obtained from different commercial sources. All solvents were used as received.

Procedures and methods. A stock solution of NIF was prepared in methanol with concentration of 1×10^{-3} M. The drug stock solution was further diluted in different neat solvents, including deionized water, methanol, ethanol, propanol, isopropanol, acetonitrile, ethylacetate, n-hexane, chloroform, 1,4-dioxane, DMF, and DMSO. Aqueous solutions were prepared using Milli-Q ultra-pure water (18 MΩ). The preparation was carried out by withdrawing a suitable volume of stock solution, evaporating methanol at room temperature, and re-dissolving the drug residues in suitable volumes of the solvents. A similar procedure was followed to prepare various solutions of hydro-organic binary systems, including water-dioxane and water-acetonitrile systems, with a v:v ratio in the range of 0–100% with an increment of 10%. The UV–Vis absorption spectra were measured using a Jasco UV-Vis spectrophotometer (USA) in 1 cm quartz cells. Within the experimental conditions, the A_{max} of all solutions obeyed to the Beer–Lambert's law.

Computational details. All DFT and TD-DFT calculations were performed using the Gaussian09 package. The DFT functional B3LYP14 coupled with the 6-31+G(d) basis set [18] was used to perform geometry optimizations in vacuo or in selected solvents, employing the integral equation formalism polarizable continuum model (IEF-PCM) [19]. The solvents chosen in this study are 1,4-dioxane, isopropanol, methanol, acetonitrile, and water. Simulated absorption spectra were obtained from the vertical electronic transition and the corresponding oscillator strength, *f*. This was calculated for the first ten excitation states, employing TD-DFT at the B3LYP/6-31+G(d) level of theory on optimized ground-state geometries.

Results and Discussion

The UV–Vis absorption spectra of NIF were measured in twelve neat solvents of different polarities and hydrogen bonding capabilities. Absorption spectra were normalized to unity; spectra measured in selected neat solvents are displayed in Fig. 1. Interestingly, the electronic absorption spectra of NIF

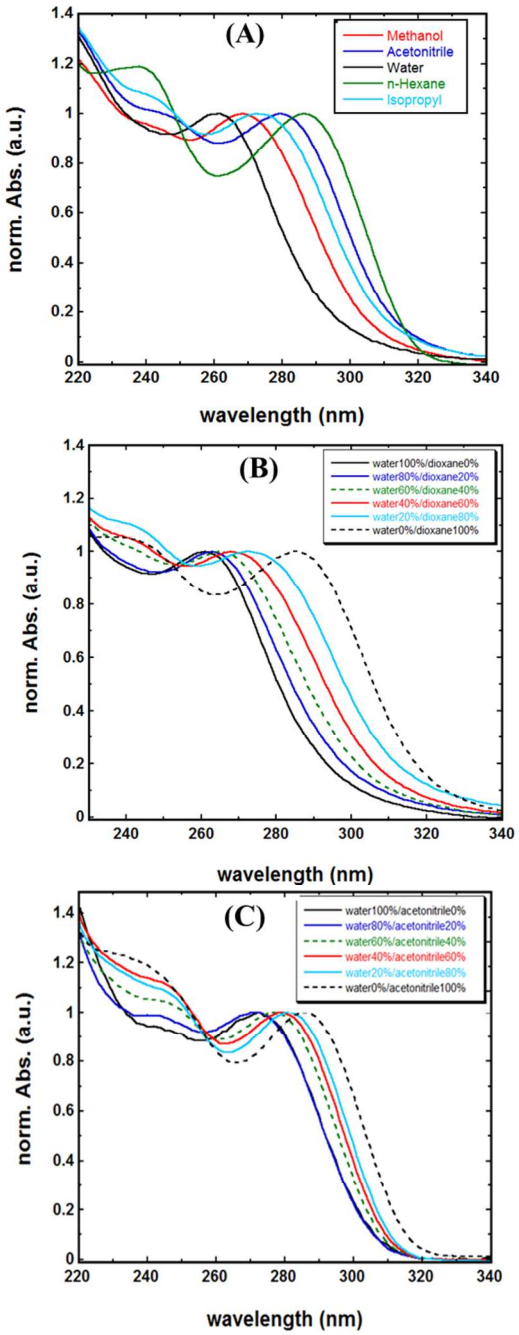

Figure 1 Normalized absorption spectra of NIF in neat solvents (A), water-dioxane mixture (B), water-acetonitrile mixture (C).

exhibit two maximum bands at ~ 240 (λ_{max2}) and 290 nm (λ_{max1}), which can be attributed to π–π*. Moreover, NIF shows a shoulder band in the range of 225 to 245 nm in all solvents except in water, ethanol, and propanol. These two bands can be attributed to π–π* within the aromatic and pyrazole moieties, respectively. While λ_{max2} exhibits a minimal solvent dependency, a notable bathochromic shift of 20–25 nm is observed for the band at λ_{max1} when increasing the polarity of the solvent; no significant change in the spectrum shape and absorbance occurred. The hypochromic shift of the main band (λ_{max1}) may indicate a higher dipole moment of the ground state compared to that of the excited state; this may cause an enhanced stabilization of the ground state in comparison to that of the excited state [20,21].

Table 1 lists the main electronic absorption properties (λ_{max1}) of NIF as well as other solvent physical properties, including refractive index (n), solvent electric permittivity (ε), orientation polarizability (Δ*f*), and Kamlet-Taft solvent parameters such as dipolarity/polarizability (π*), hydrogen-bond donating (α) and accepting (β) capability.

Table 1. Physical parameters of solvents and the corresponding λ_{max} of NIF [9,22,23].

Solvent	ε	n	Δ*f*	π*	α	β	λ_{max1} (nm)
polar protic							
water	78.4	1.333	0.320	1.09	1.17	0.18	262
methanol	32.7	1.329	0.310	0.60	0.93	0.62	268
ethanol	24.6	1.361	0.289	0.54	0.83	0.77	272
propanol	20.8	1.386	0.274	0.52	0.78	0.85	273
isopropanol	19.9	1.378	0.276	0.48	0.76	0.95	272
polar protic							
acetonitrile	36.6	1.344	0.305	0.75	0.19	0.31	279
DMSO	46.5	1.477	0.264	1.00	0	0.76	283
DMF	36.7	1.431	0.276	0.87	0	0.69	283
ethylacetate	6.1	1.372	0.200	0.55	0	0.45	284
nonpolar							
chloroform	4.8	1.446	0.153	0.58	0.44	0.00	282
1,4-Dioxane	2.2	1.422	0.022	0.55	0	0.37	285
n-hexane	1.9	1.375	0.002	- 0.08	0	0	287

In order to understand the solvatochromic behaviour of the studied drugs, the electronic absorption spectroscopic properties were studied as a function of solvent polarity. First, the absorption maximum wavenumber (ν_{max}) of NIF was plotted as a function of the orientation polarizability, Δ*f* (ε, n) [24]:

$$\Delta f = \frac{\varepsilon-1}{2\varepsilon+1} - \frac{n^2-1}{2n^2+1} \quad (1)$$

Fig. 2-A displays the correlation between the Δ*f* and ν_{max} of NIF in solvents of different polarity. Although no correlation between ν_{max} and Δ*f* for the studied solvents was found, two subregions could be identified that contain protic or aprotic solvents. Thus, if one considers only protic solvents, a satisfactory linearity occurs, with a regression coefficient (R) equal to 0.93. No linear correlation was found for the other solvents. These results indicated that both the solvent polarization and the hydrogen bonding play a major role in determining the observed solvatochromic behaviour of NIF. Furthermore, the positive slope obtained for the protic solvents suggest that the energy required for solvation is negative and specific interactions, such as dipole–dipole and hydrogen bonding, between the drug and the solvents occur.

The dual effect of solvent polarity and hydrogen bonding capability was further investigated via absorption spectra in binary hydro-organic systems, such as water-1,4-dioxane (W-D), and water-acetonitrile (W-A) binary systems (Fig. 1-B and Fig. 1-C, Table 2). We would like to remark that the solvatochromic parameters of these mixtures were taken from previous studies [25-29].

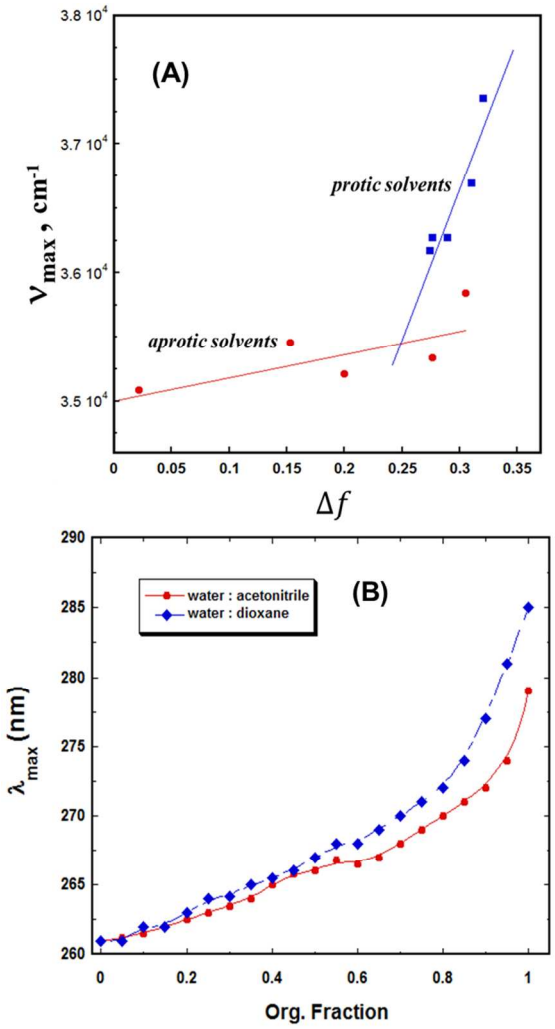

Figure 2. (A) Variation in absorption λ_{max} of NIF with orientation polarizability (Δ*f*); (B) variation in λ_{max} of NIF with organic content in hydroorganic binary systems.

Similarly to neat solvents, Fig. 1-B and Fig. 1-C show that no linear correlation occurs between λ_{max1} and the content of water in both binary systems, confirming that that the polarity of the medium is not the only factor that affects the λ_{max1} of NIF. The absorption spectrum of NIF exhibits a λ_{max1} of 262 and 285 nm in water and 1,4-dioxane, respectively, the spectral shift being equal to 23 nm. This can be compared to a spectral shift of 15 nm of the NIF absorption spectrum in the W-D mixture with a water content of 10%. The ~ 35% reduction in the spectral shift provides further evidence for the hydrogen bond character of the main band in protic solvents [10], which is also consistent with our results obtained from the neat solvents studies.

Table 2. Summary of solvatochromic parameters of hydro-organic binary systems and the corresponding λ_{max} of NIF [23-27].

H_2O content %	π*		α		β		λ_{max} (nm)	
	W : A	W : D	W : A	W : D	W : A	W : D	W : A	W : D
100	1.09		1.17		0.47		261	
90	1.08	1.14	1.05	1.06	0.61	0.51	262	262
80	0.97	1.12	0.96	0.92	0.61	0.54	263	263
70	0.92	1.09	0.92	0.82	0.61	0.56	264	265
60	0.87	1.05	0.89	0.77	0.6	0.59	265	266
50	0.85	0.99	0.86	0.73	0.59	0.61	266	267
40	0.82	0.92	0.83	0.6	0.59	0.63	267	268
30	0.8	0.85	0.78	0.52	0.59	0.63	268	270
20	0.77	0.78	0.7	0.38	0.57	0.61	270	272
10	0.75	0.7	0.55	0.2	0.53	0.54	272	277
0	0.73	0.54	0.25	0.02	0.47	0.42	279	285

A multiple linear regression analysis (MLRA) based on the Kamlet-Taft equation was performed in order to further investigate the solvent-solute interactions. This equation has been effectively applied to separate the influence of non-specific chemical interactions, including electrostatic effects (dipolarity/polarizability), from specific interactions, including hydrogen bonding, which in turn are correlated to the molecular structure of a compound. The Kamlet-Taft equation is expressed as [22,23]:

$$\nu_{max} = \nu_o + a\alpha + b\beta + c\pi^* \quad (2)$$

where ν_{max} is the wavenumber (cm^{-1}) in the maximum absorption band of the investigated compounds in different solvents; νo is the regression intercept, which corresponds to the gaseous phase; α reflects the hydrogen-bond donor acidity (HBD); β reflects hydrogen-bond acceptor basicity (HBA); π*, an index of the dipolarity-polarizability of the solvent, reflects the ability of the solvent to stabilize a dissolved charge or dipole; ν_o, a, b, c are independent constants, and their magnitudes and sign provide a measure of the influence of the corresponding solute-solvent interactions on the absorption maximum wavenumber. The MLRA was performed for the three systems, namely neat solvents, W-D and W-A binary systems described in Equations 3, 4, and 5, respectively:

$$\nu_{max} = (34783 \pm 211) + (2140 \pm 193)\alpha + (42 \pm 263)\beta + (580 \pm 286)\pi^* ; \quad R = 0.97 \quad (3)$$

$$\nu_{max} = (33303 \pm 282) + (1779 \pm 304)\alpha + (1986 \pm 430)\beta + (1813 \pm 557)\pi^*; R = 0.99 \quad (4)$$

$$\nu_{max} = (33623 \pm 693) + (2351 \pm 368)\alpha + (2176 \pm 873)\beta + (835 \pm 680)\pi^* ; R = 0.99 \quad (5)$$

The obtained values of the correlation coefficients (R) for the investigated solvents show a high correlation and confirm that these equations can be employed to further investigate the solute-solvent interactions between NIF and the studied solvents. In particular, the influence of the hydrogen-bond capability of the solvent is a dominant factor that affects the position of the peak λ_{max1} of NIF with contribution levels of ~79%, 68%, 84% for neat solvents, W-D, and W-A systems, respectively. Thus, the Kamlet-Taft equation provides a better description for the solvent effect on the absorption spectral properties of NIF, in comparison to the correlation between the Δf and ν_{max}.

The practical applicability of equations 3, 4, and 5 was tested by using them to verify the correlation between the measured and calculated values of ν_{max}. Fig. 3 illustrates these correlations for NIF in the tested systems. Excellent correlations between the experimental and calculated values have been established,with correlation coefficients >0.99,

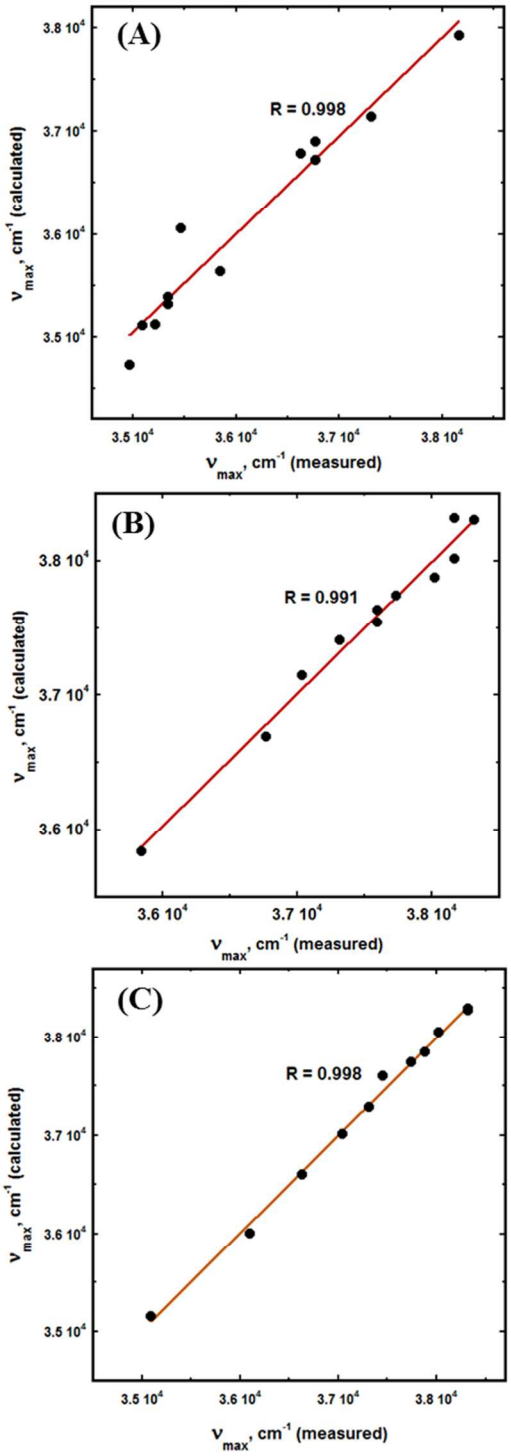

Figure 3. Comparison between measured and calculated ν_{max} NIF in neat solvents (A), a water-dioxane mixture (B), and a water-acetonitrile mixture (C).

which indicates the practicality of employing the Kamlet-Taft procedure in interpreting and correlating the solvatochromic shifts of the NIF. As mentioned above, a significant solvatochromic shift is observed within the electronic absorption band that corresponds to $\pi-\pi^*$ transitions. This absorption spectral change indicates that these transitions may be affected by solute-solvent interactions, which are likely to be relevant factors that influence the final geometry of NIF. Although no clear evidence was found, we believe that the delocalization of electron density may contribute further stabilization to the ground state of the Pyrazole drugs, which in turn could rationalize the large solvatochromic shifts in their electronic absorption spectra. This hypothesis was examined through DFT calculations.

Computational investigations: molecular geometry. The optimized geometry of NIF obtained at the DFT/6-31+G(d) level in vacuo and in water is displayed in Fig. 4. The positive harmonic vibrational frequencies indicate that the optimized structures were minima. Relevant computed structural parameters in selected solvents along with the corresponding experimental X-ray crystallographic data of NIF are listed in Table 3 [30]. Structural parameters in all the other solvents are shown in Table S1. Our data showed that DFT calculations well reproduced the available experimental data [30].

However, some variations can still be noted; this includes some dihedral angles. It was experimentally reported using X-ray crystallographic data that O2 and N2 of NIF are involved in intermolecular hydrogen bonding, which could presumably explicate such variations. As shown in Fig. 4, in order to achieve stronger intermolecular hydrogen bonding, the skeleton of NIF is made planar in vacuo. In a polar environment instead, the amide group together with the pyridine moiety is out of the plane of the pyrazole and the phenyl rings.

Table 3. Selected experimental and calculated (at the B3LYP/6-31G+(d) level of theory) structural parameters of NIF in different solvents [30]

Geometric parameters	Exp.*	Calculated (DFT//B3LYP/6-31G+(d) level)					
		Vacuo	Water	MeOH	AcNT	Isoprop.	Dioxane
Bond Length (Å)							
O(1)-C(6)	1.229	1.230	1.235	1.234	1.235	1.234	1.232
N(2)-C(6)	1.349	1.373	1.371	1.372	1.372	1.372	1.373
N(3)-N(4)	1.396	1.414	1.411	1.411	1.411	1.411	1.413
O(2)-C(9)	1.229	1.233	1.241	1.240	1.241	1.240	1.236
N(2)-C(7)	1.415	1.399	1.410	1.409	1.408	1.408	1.402
N(3)-C(8)	1.352	1.409	1.376	1.377	1.379	1.381	1.402
N(3)-C(11)	1.464	1.473	1.468	1.468	1.468	1.468	1.472
N(4)-C(9)	1.410	1.394	1.405	1.405	1.404	1.404	1.395
C(7)-C(8)	----	1.366	1.372	1.371	1.371	1.370	1.367
Bond Angle (°)							
C(6)-N(2)-C(7)	119.3	129.3	123.8	123.8	124.3	124.3	128.0
N(4)-N(3)-C(8)	108.1	107.0	107.2	107.2	107.2	107.2	107.0
C(9)-N(4)-N(3)	108.2	109.6	109.3	109.3	109.3	109.3	109.6
O(1)-C(6)-N(2)	121.5	123.3	122.8	122.8	122.8	122.8	123.2
C(8)-C(7)-N(2)	126.2	136.4	127.7	127.8	128.5	128.7	134.6
C(9)-C(7)-N(2)	124.5	114.8	123.4	123.2	122.6	122.4	116.5
C(10)-C(8)-N(3)	121.6	118.5	121.6	121.6	121.4	121.3	119.2
N(4)-C(9)-C(7)	104.8	105.4	104.6	104.6	104.6	104.7	105.2
C(7)-N(2)-C(6)-O(1)	2.8	-2.9	-3.5	-4.1	-4.0	-4.6	-4.6
Dihedral angle (°)							
C(6)-N(2)-C(7)-C(8)	103.0	22.8	68.4	67.2	59.1	58.0	33.4
C(6)-N(2)-C(7)-C(9)	-68.0	-156.2	-108.0	-109.1	-117.9	-118.9	-146.3
N(3)-N(4)-C(9)-O(2)	172.3	174.5	171.7	171.8	172.0	172.2	174.2
N(3)-N(4)-C(9)-C(7)	-5.7	-3.8	-6.8	-6.8	-6.7	-6.6	-4.4
C(8)-C(7)-C(9)-O(2)	-175.1	-177.9	-175.9	-176.0	-176.4	-176.6	-178.0
C(8)-C(7)-C(9)-N(4)	2.6	0.4	2.6	2.5	2.2	2.1	0.5

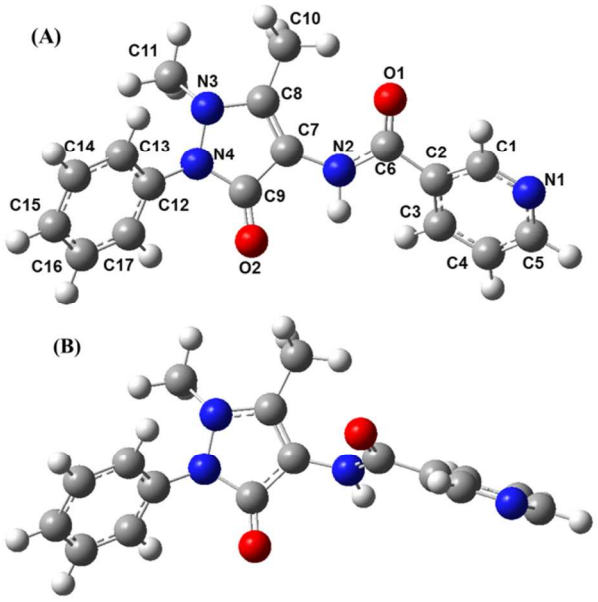

Figure 4. DFT B3LYP/6-31G+(d) optimized molecular geometry of NIF in vacuo (A) and in water (B). Atoms numbering is also displayed.

The degree of electron density delocalization of the amide group, bridging the pyridine and the pyrazole rings, is hardly affected by solvation. In contrast, a change of the electron density delocalization is observed within the pyrazole ring, suggesting a potential charge transfer in the direction N3→C8→C7→C9→O2 through single-double bond conjugation. This can be deduced from the bond length of the atoms involved. The N3-C11 bond length (1.464 Å) hardly changed upon solvation, whereas the bond length of N3-C8 (1.376 Å obtained in water from DFT calculation), C7-C8 (1.366 Å), C7-C9 (1.446 Å), and C9-O2 (1.233 Å) increase when the polarity of the solvent decreases. Further, the Mulliken charges for all non-H atoms are listed in Table S2. These data showed a significant variation in the atomic charges of some atoms in different solvents of different polarity. For example, O2 exhibits higher negative atomic charges in polar solvents in comparison with non-polar solvents, e.g., -0.621 and -0.533 1,4-dioxane, respectively. This is consistent with the proposed charge delocalization across the pyrazole ring.

Energy levels and Absorption spectra.

It is worth to mention that computational chemical models can be employed for providing insights into interpretation of experimental findings. Hence, theoretical reproducing of experimental results is valuable for accomplishing such objectives. TD-DFT, associated with different functionals, is the most effective approach for the theoretical investigation of optical properties of various types of materials, including medium to large size organic molecules. In particular, TD-DFT is typically employed with PCM to investigate such optical properties in solution. However, PCM may neglect specific solvent-solute interactions, such as hydrogen bonding. This can lead to a significant error in the simulated optical properties of a material of interest. Thus, the choice of suitable computational models and functionals is crucial in reproducing the experimental spectra [31,32]. Simulated electronic

absorption spectra of NIF in different solvents were obtained via TD-DFT calculations coupled with IEFPCM models. Two DFT functionals were employed, namely B3LYP and CAM-B3LY with the 6-31G+(d) basis set. For the sake of simplicity, theoretical λ_{max} is defined as the wavelength of HOMO→LUMO transition. Interestingly, CAM-B3LYP reproduced well the NIF absorption spectra in ten different solvents (Fig. 5-A); the relative oscillator strength for each transition is represented by vertical lines. In contrast, B3LYP poorly reproduced NIF absorption spectra in five selected solvents with an average overestimation $\lambda_{max}^{theor} - \lambda_{max}^{expt}$ of ~ 50 nm (Fig. S1). It can be noticed that not only did CAM-B3LYP well reproduce the absorption spectra of NIF in solution, but it also described the negative solvatochromism (Fig. 5-B). Fig. 6 illustrates a comparison between the experimental and theoretical (CAM-B3LYP/6-31G+(d)-IEFPCM) λ_{max} in different solvents. Notably, an average underestimation ($\lambda_{max}^{expt} - \lambda_{max}^{theor}$) of ~ 11 nm was determined; thus, the results obtained from our TD-DFT calculations are within the error expected for this approach as compared with reported results of other molecules [31-35].

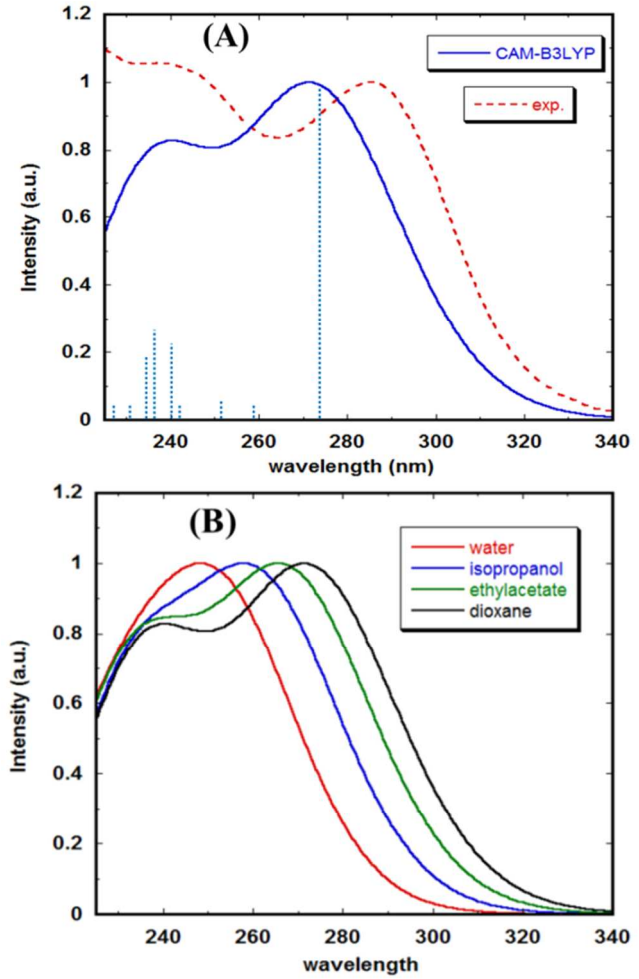

Figure 5. Experimental and simulated electronic absorption spectra of NIF in 1,4-dioxane (A); simulated electronic absorption spectra of NIF in selected solvents (B). Vertical lines in (A) represent the relative oscillator strength of each transition.

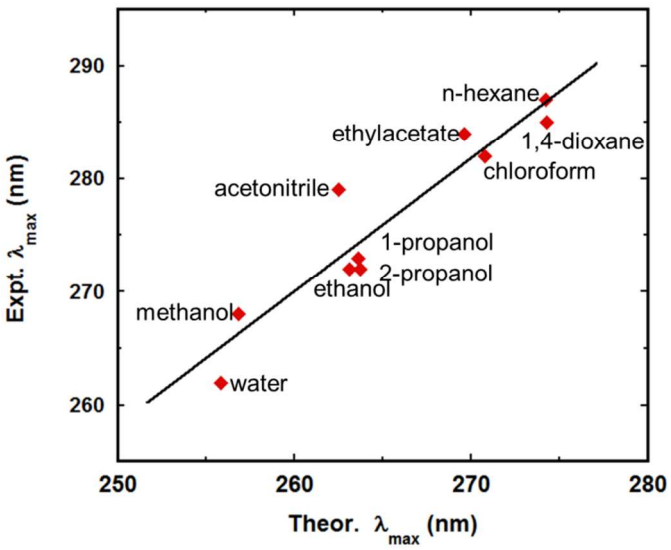

Figure 6. Comparison between experimental and theoretical λ_{max} obtained at the CAM-B3LYP (6-31G+(d))-IEFPCM level of theory in different solvents.

The effect of solvent polarity on the frontier orbitals (HOMO, LUMO) and their corresponding energy gaps were examined. Obtained results are displayed in Fig. 6, and data collected in Table 4. As expected, the HOMO and LUMO orbitals of the amide group are distributed over the pyrazole and pyridine rings, respectively. As discussed earlier, our DFT calculations suggested that the electron density delocalization of the pyrazole ring is facilitated in polar solvents. This effect is likely due to the stabilization of the HOMO orbital. The electron density distribution of the LUMO over the pyridine ring is hardly affected, mirroring the structural properties of this group, which also hardly change upon solvation. Interestingly, the oscillator strength is significantly enhanced for the HOMO→LUMO transition by a decrease in the polarity of the solvent. This is likely due to a reduced HOMO-LUMO gap related to a polarity decrease, which in turn accounts for bathochromic shift observed in NIF absorption spectra upon decreasing the medium polarity. In general, the bathochromic shift can be calculated employing the following equation:

$$\Delta\lambda = \lambda_{max}^{solvent} - \lambda_{max}^{water} \quad (6)$$

Table 4. Selected computed energetic and spectral properties of NIF in different solvents obtained at the CAM-B3LYP/6-31G+(d) level of theory.

Property		Vacuo	Water	EthOH	2-PrOH	Chloroform	Dioxane
LUMO (eV)		-0.0210	-0.0195	-0.0200	-0.0200	-0.0202	-0.0206
HOMO (eV)		-0.2731	-0.2808	-0.2776	-0.2774	-0.2743	-0.2730
ΔE (eV) (E_{LUMO}-E_{HOMO})		0.2521	0.2613	0.2576	0.2574	0.2541	0.2524
Δλ (nm)	expt.	----	0	10	10	20	23
	theor.	16	0	7	8	15	19
$\Delta G_{Solvation}$ (cal.mol^{-1})		0	-22.2	-21.3	-20.64	-14.35	-7.67
Dipole moment (Debye)		4.843	10.37	9.16	9.00	7.19	5.98

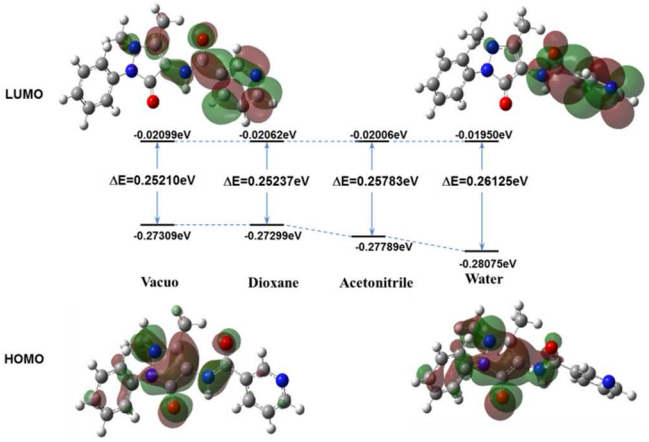

Figure 7. Ground-state optimized geometry of NIF in different media; HOMO, LUMO and their corresponding energy gaps obtained at the B3LYP/6-31G+(d) level of theory.

Additional features (dipole moment, solvation energy)

Solvation exerts a notable influence also on the IR spectra of NIF, which were calculated in vacuo and in water (Fig. S2). For instance, typical C=O stretching frequencies of 1724 and 1743 cm^{-1} were obtained for the amide (C6=O1) and pyrazole (C3=O6) carbonyl, respectively, in vacuo, to compare with the corresponding values of 1702 and 1687 cm^{-1} in water. Polarity instead showed only a minor effect.

Dipole moments and solvation energies (ΔG_{solv}) are listed in Table 4. In particular, DFT calculations show that the dipole moment of the ground state increases with the polarity of the solvent, e.g., an increase of ~ 4 Debye is observed form 1,4-dioxane to water. This can be attributed to the stabilization of charge separation in polar solvents, which is consistent with the results obtained from the electron density distribution of the frontier orbitals. Solvation free energy (ΔG_{solv}) of drugs is an important thermodynamic parameter that contributes to the drug activity [36]. Similarly, ΔG_{solv} increases with the polarity of the solvent. Stabilization of charge separation may lead to stronger solvent–solute interactions and consequently increased ΔG_{solv}.

Conclusions

The electronic spectral, solvatochromic, and geometrical properties of NIF, a pyrazole-nicotinamide drug, were explored through a combination of experimental and computational methods. A negative solvatochromism of NIF was observed upon increasing the solvent polarity. The spectral shifts in the electronic absorption spectra of NIF were quantitatively described by two solvatochromism models, which include the orientation polarizability (Δf) and the Kamlet-Taft solvent parameters, comprising π* (dipolarity/polarizability), α (hydrogen bond donating capacity) and β (hydrogen bond accepting ability). Our data showed that the major contributions to the solvatochromic behaviour of NIF are the polarity of the medium, its hydrogen bonding capability, and potential delocalization of electron density, which is facilitated in polar solvents. Density functional theory (DFT) and time-dependent DFT (TD-DFT) calculations at the CAM-B3LYP/6-31G+(d) level of theory coupled with integral equation formalism polarizable continuum model (IEF-PCM) have well reproduced the experimental findings. Thus, determination of the solvatochromic behaviour of different drugs, such as pyrazole-nicotinamide, may provide a valuable tool for the interpretation of their spectroscopic properties and the understanding of their chemical behaviour in different conditions.
This study is expected to provide valuable information for further development and formulation of such drugs and their potential for pharmaceutical applications.

Acknowledgements

This work was partially financed by Qatar University and Taibah University.

.

Notes and references

[a] Department of Chemistry & Earth Sciences, College of Arts & Sciences, Qatar University, P.O. Box 2713, Doha, State of Qatar.
.* abdulilah.baniyaseen@qu.edu.qa
[b] Department of Chemistry, Faculty of Science, Taibah University Al-Madinah Al-Munawwarah, Saudi Arabia.

1 M. Serrentino, A. Catalfo, A. Angelin, G. Guidib and E. Sage, *Mutat. Res.*, 2010, **692**, 34.

2 M. Quintero, *ARS Pharmaceutica*, 2000, **41**, 27.

3 J. Serrano-Perez, L. Serrano-Andres and M. Merchan, *J. Chem. Phys.*, 2008, **347**, 422.

4 M. Budai, Z. Szabo, I. Voszka, P. Maillard, G. Csık and P. Grof, *Chem. Phys. Lipids*, 2007, **145**, 63.

5 S. Jantova, K. Konarikova, S. Letašiova, E. Paulovicova, V. Milata and V. Brezova, *J. Photoch. Photobio. B*, 2011, **102**, 77.

6 C.S. Oliveira,; R. Turchiello, A.J. Kowaltowski, G.L. Indig and M.S. Baptista, *Free Radical Bio. Med.*, 2011, **51**, 824.

7 Y. Gulsevena, E. Tasxala, I. Sıdıra, T. Gungorb, H. Berberc and C. Ogretird, *Int. J. Hydrogen Energ.*, 2009, **34**, 5255.

8 M. Orozco and F.J. Luque, *Chem. Rev.*, 2000, **100**, 4187.

9 C. Spies, B. Finkler, N. Acarb and G. Jung, *Phys. Chem. Chem. Phys.*, 2013, **15**, 19893.

10 C. Reichardt, *Chem. Rev.*, 1994, **94**, 2319.

11 A.D. Bani-Yaseen, *J. Fluoresc.*, 2012, **21**, 1061.

12 C. Reichardt and T. Welton, Solvents and Solvent Effects in Organic Chemistry, 4th ed., Wiley-VCH: Weinheim, Germany, 2011.

13 A. Marini, A. Munoz-Losa, A. Biancardi and B. Mennucci, *J. Phys. Chem. B*, 2010, **114**, 17128.

14 A. Mota, J.P. Hallett, M.L. Kuznetsov and I. Correia, *Phys. Chem. Chem. Phys.*, 2011, **13**, 15094.

15 F.D. Hart and P.L. Boardman, *Brit Med. J.*, 1964, **5397**, 1553.

16 H.-S. Shin, B.-B. Park, S.N. Choi, J.J. Oh, C.P. Hong and H. Ryu, *J. Anal. Toxicol.*, 1998, **22**, 55.

17 T.J. Kamerzell, R. Esfandiary, S.B. Joshi, C.R. Middaugh and D. Volkin, *Adv. Drug Deliver. Rev.*, 2011, **63**, 1118.

18 M.J. Frisch, G.W. Trucks, H.B. Schlegel, G.E. Scuseria, M.A. Robb, J.R. Cheeseman, G. Scalmani, V. Barone, B. Mennucci, G.A. Petersson, H. Nakatsuji, M. Caricato, X. Li, H.P. Hratchian, A.F. Izmaylov, J. Bloino, G. Zheng, J.L. Sonnenberg, M. Hada, M. Ehara, K. Toyota, R. Fukuda, J. Hasegawa, M. Ishida, T. Nakajima, Y. Honda, O. Kitao, H. Nakai, T. Vreven, J.A. Montgomery, Jr., J.E. Peralta, F. Ogliaro, M. Bearpark, J.J. Heyd, E. Brothers, K.N. Kudin, V.N. Staroverov, R. Kobayashi, J. Normand, K. Raghavachari, A. Rendell, J.C. Burant, S.S. Iyengar, J. Tomasi, M. Cossi, N. Rega, J.M. Millam, M. Klene, J.E. Knox, J.B. Cross, V. Bakken, C. Adamo, J. Jaramillo, R. Gomperts, R.E. Stratmann, O. Yazyev, A.J. Austin, R. Cammi, C. Pomelli, J.W. Ochterski, R.L. Martin, K. Morokuma, V.G. Zakrzewski, G.A. Voth, P. Salvador, J.J. Dannenberg, S. Dapprich, A.D. Daniels, Ö. Farkas, J.B. Foresman, J.V. Ortiz, J. Cioslowski, and D.J. Fox, Gaussian 09, Revision A.1, Gaussian, Inc., Wallingford CT, 2009.

19 J. Tomasi, B. Mennucci and E. Cancès, *J. Mol. Struct. (Theochem)*, 1999, **464**, 211.

20 C. Garcıa, R. Oyola, L. Pinero, D. Hernandez and R. Arce, *J. Phys. Chem. B*, 2008, **112**, 168.

21 H.-R. Park, C.-H. Oh, H.-C. Lee, S.R. Lim, K. Yang and K.-M.Bark, *Photochem. Photobiol.*, 2004, **80**, 554.

22 M.J. Kamlet, J.L.M. Abboud, M.H. Abraham and R.W. Taft, *J. Org. Chem.*, 1983, **48**, 2877.

23 C. Laurence, P. Nicolet, M. T. Dalati, J. M. Abboud and R. Notario, J. Phys. Chem, 1994, 98, 5807.

24 J.R. Lakowicz, Principles of fluorescence spectroscopy, 3rd ed.; Kluwer Academic/Plenum Press, New York, 2006.

25 M. Tadeus, I.M. Krygowsk and K. Pioter, *Tetrahydron*, 1985, **20**, 4519.

26 Y. Marcus, *J. Chem. Soc., Perkin Trans.*, 1994, **2**, 1751.

27 E. Casassas, G. Fonrodona and A. de Juan, *Inorg. Chim. Acta*, 1991, **187**, 187.

28 W.J. Cheong and P.W. Carr, *Anal. Chem.*, 1988, **60**, 820.

29 A J.H. Park, M.D. Jang and D.S. Kim, *J. Chromatogr.*, 1990, **513**, 107.

30 R. Tanaka, K. Horio, M. Haramura and A. Tanaka, *X-ray Struct. Anal. Online*, 2004, **20**, x171.

31 A. Pedone, *J. Chem. Theory Comput.* 2013, **9**, 4087.

32 L. Bernasconi and E.J. Baerends, *J. Am. Chem. Soc.*, 2013, **135**, 8857. ,

33 A. Pedone, J. Bloino, S. Monti, G. Prampolinib and V. Barone, *Phys. Chem. Chem. Phys.*, 2010, **12**, 1000.

34 C. Joamorski-Jodicke and M. E. Casida, *J. Phys. Chem. B*, 2004, **108**, 7132.

35 P. Kar, R. Lipowsky and V. Knecht, *J. Phys. Chem. B*, 2013, **117**, 5793.

36 S.A. Martins and S. F. Sousa, *J. Comput. Chem.* 2013, **34**, 1354.

